Applied Physics Letters

Maximal absorption in ultrathin TiN films for microbolometer applications

Cite as: Appl. Phys. Lett. **121**, 234101 (2022); https://doi.org/10.1063/5.0123671
Submitted: 31 August 2022 • Accepted: 23 November 2022 • Published Online: 06 December 2022

Ting S. Luk, Guangping Xu, Willard Ross, et al.

COLLECTIONS

Paper published as part of the special topic on Thermal Radiation at the Nanoscale and Applications

View Online

Export Citation

CrossMark

ARTICLES YOU MAY BE INTERESTED IN

Wideband mid infrared absorber using surface doped black silicon
Applied Physics Letters **121**, 231703 (2022); https://doi.org/10.1063/5.0117289

Solution processed organic thermoelectric generators as energy harvesters for the Internet of Things
Applied Physics Letters **121**, 230501 (2022); https://doi.org/10.1063/5.0129861

Ion transfer into solution-processed electrodes can significantly shift the p–n junction and emission efficiency of light-emitting electrochemical cells
Applied Physics Letters **121**, 231102 (2022); https://doi.org/10.1063/5.0123469

QBLOX

Integrates all Instrumentation + Software for Control and Readout of **Spin Qubits**

visit our website >

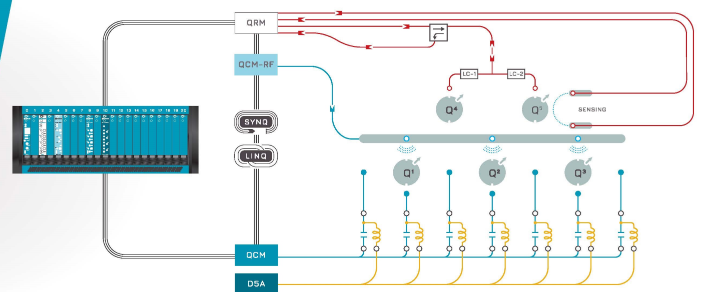

AIP Publishing

© 2022 Author(s).

Applied Physics Letters ARTICLE scitation.org/journal/apl

Maximal absorption in ultrathin TiN films for microbolometer applications

Cite as: Appl. Phys. Lett. **121**, 234101 (2022); doi: 10.1063/5.0123671
Submitted: 31 August 2022 · Accepted: 23 November 2022 ·
Published Online: 6 December 2022

Ting S. Luk,[1,a)] Guangping Xu,[2] Willard Ross,[1] John N. Nogan,[1] Ethan A. Scott,[1] Sergei Ivanov,[1] Oana Niculescu,[3] Oleg Mitrofanov,[4] and C. Thomas Harris[1]

AFFILIATIONS

[1]Center for Integrated Nanotechnologies, Sandia National Laboratories, Albuquerque, New Mexico 87185, USA
[2]Geochemistry Department, Sandia National Laboratories, Albuquerque, New Mexico 87185, USA
[3]Department of Engineering, University of Cambridge, Cambridge, Cambridgeshire CB3 0FA, United Kingdom
[4]Electronic and Electrical Engineering Department, University College London, London WC1E 7JE, United Kingdom

Note: This paper is part of the APL Special Collection on Thermal Radiation at the Nanoscale and Applications.
[a)]**Author to whom correspondence should be addressed:** tsluk@sandia.gov

ABSTRACT

Ultrathin light absorbers present a viable route toward improving the specific detectivity and response time of microbolometers. However, for an ultrathin film to absorb light efficiently, the dielectric function of the film and its thickness must satisfy strict requirements. We experimentally demonstrate an average absorptance of 48% $\pm$ 2.5% in the 8–13 μm (769–1250 cm^{-1}) spectral range for 10 nm thick titanium nitride (TiN), a value bordering on the 50% fundamental absorptance limit for a suspended thin film. The heat capacity per unit area of this absorber is only 1.2×10^{-6} J/K/cm^2, which is beneficial for improving the response time of a microfabricated bolometer. We also show that a sufficient condition for reaching maximal absorption in an ultrathin film is that $\varepsilon'' \gg |\varepsilon'|$.

Published under an exclusive license by AIP Publishing. https://doi.org/10.1063/5.0123671

Bolometers have proven to be an effective, low-cost alternative to semiconductor photovoltaic sensors for mid- and long-wavelength infrared (IR) thermal imaging and remote sensing applications.[1] While the specific detectivity (see Fig. S7 in the supplementary material) of an ideal photovoltaic detector is approximately 2.5× higher than that of an ideal room temperature bolometer at 12 μm, in many instances, the cost and resource overhead associated with this benefit may seem unwarranted.[2] However, certain thermal sensing applications do exist where the available maximum detectivity must be selected, regardless of size, weight, and power requirements. Thus, a strong technological need indeed remains to improve upon the performance of bolometers.

One of the principal elements in a bolometer is the absorber, which collects infrared radiation to produce a temperature rise. Naturally, a material with a higher absorption coefficient consisting of a relatively smaller thermal mass will produce a larger temperature rise in a shorter amount of time. Commercial bolometers rely on anti-reflection coatings and relatively thick (250–500 nm) silicon nitride (SiN) as an absorber for long-wavelength infrared (LWIR) radiation. A viable route toward improving detector performance relies upon scaling the bolometer to smaller dimensions to reduce its thermal conductance and its thermal mass to the extent that the heat loss is dominated by radiation rather than conduction, improving both detectivity and response time.[2] However, when scaling the bolometer platform to thickness dimensions well below 250 nm, the SiN platform can no longer be used effectively as an absorbing medium (see Fig. S6 in the supplementary material), and an additional material must be integrated into the system to collect light. When pursuing this down-scaling strategy, having a strong absorber with a thickness comparable to or well below the platform itself allows one to maintain a thin aspect ratio in the device while also providing a small thermal mass. This approach of engineering strong absorption[3] and a smaller thermal mass simultaneously in an ultra-thin film material can ultimately improve bolometer performance[4–6] (Fig. S7 in the supplementary material).

From the perspective of light collection, perfect (100%) or near perfect absorption of a plane wave in an optically thin material is ideal and has been explored extensively.[7–24] However, in a typical IR bolometer, the absorber element is thermally isolated from the environment (i.e., suspended) resulting in an ambient index of refraction of 1, which limits maximum absorption within this thin film system for single-port excitation to 50%. Furthermore, thermal radiation is typically

Published under an exclusive license by AIP Publishing

unpolarized and broadband, and thus, schemes that can achieve perfect absorption but require a specific polarization are not compatible with the design of a traditional bolometer.

In the 1950s, researchers recognized that the 50% limit of absorptance could be attained using thin, free-standing metallic films if the imaginary permittivity were much greater than its real part. We refer to this condition as maximal absorptance (MA).[25,26] Consider, for example, a bolometer with a metallic thin film absorber scaled to relatively small dimensions (e.g., ~10 nm thick), where the thermal conductance of this bolometer platform has been reduced by 100 times and its thermal response is 100 times faster than a standard commercial bolometer. If this bolometer's maximum absorption is limited by the fundamental 50% absorption limit but a substantial reduction in thermal conductance and thermal mass can be achieved, then the trade-off with lower absorptance ultimately becomes advantageous (see the supplementary material). Here, we show that a simple sputter-deposited TiN film can simultaneously achieve high absorptance, low thermal conductance, and low thermal mass and can be supported by a very thin film of SiN (20–100 nm). We demonstrate an ultralow thermal mass broadband absorber comprised of a 10 nm thick TiN film that possesses a heat capacity per unit area of 1.2 μJ/K/cm^2, a value similar to state-of-the-art ultrathin absorbers formed using a precisely engineered 4 nm Au/CuO layer.[27] We measure the average absorptance of this TiN film to be 48% in the spectral region of 8–13 μm, achieving the MA within our measurement uncertainty. These results provide a pathway to achieve low thermal mass and low thermal conductance room temperature bolometers using simple and inexpensive fabrication methods.

Thin film absorptance (A) can be calculated from reflectance (R) and transmittance (T) of the film stack structure by virtue of $A = 1 - R - T$. For a free standing metallic thin film, the required condition for maximal absorptance[25] is $\sigma d Z_0 = 2$, a condition that the film impedance is half of the free-space impedance, where σ is the conductivity of the film, d is the thickness of the film, and Z_0 is the free-space impedance. With the assumption $\varepsilon' = 0$, the maximal absorption condition for ε'' is $\varepsilon'' = \frac{\sigma}{2\omega\varepsilon_0}$, where ε' and ε'' are the real and imaginary parts of the thin film permittivity, respectively, and ε_0 is the vacuum permittivity. Using the bulk conductivity of a metal such as Au, the required thickness for MA is 0.1 nm, which is well below the threshold of forming a continuous film. Furthermore, when a supporting thin film layer is added to the absorbing film, the analytical solution for the required permittivity for MA becomes non-trivial.[12,22,28] Using the transfer matrix method (see the supplementary material), we explored the required permittivity values for MA in films with thickness of order 10 nm. Consistent with previous findings, we obtain the condition for MA is $\varepsilon'' \gg |\varepsilon'|$, and simultaneously $\varepsilon'' \gg 1$. We also show that the real part of the permittivity ε' does not need to be negative (metallic) for MA to occur. Based on the published work,[29] we chose TiN as a candidate to satisfy the foregoing requirements. We will show later that by using a lossy metal, such as TiN with a thickness of ~10 nm, MA can be achieved. It is worth noting that typical low loss metals have the property $|\varepsilon'| \gg \varepsilon''$; therefore, the MA condition cannot be easily met for infrared wavelengths.[28]

To realize this absorber scheme, we deposited TiN by sputtering on a suspended, 100 nm thick, 500 × 500 μm^2 SiN membrane. An optical microscope image of the membrane before deposition is shown in Fig. S1(a) in the supplementary material. The deposition times for samples A, B, C, and D were 400, 525, 700, and 1000 s, respectively. For each deposition run, there were two membrane samples for redundancy and one witness sample, all placed within 2–3 cm of each other to ensure a common deposition condition. The witness sample substrates were silicon coated with 24 nm of SiN to ensure similar adhesion and relaxation properties. These films as deposited exhibited compressive stress as evidenced by the highly wrinkled SiN membrane shown in Fig. S1(b). However, upon rapid annealing at temperatures of 750 °C or higher in forming gas for 30 s, these films relaxed to a no-wrinkle state [Fig. S1(c)]. Using atomic force microscopy, we established that even the thinnest film (sample A) is continuous with a root mean square roughness of 0.5 nm [Fig. S1(d)]. X-ray diffraction measurements of the witness sample confirmed that these films were non-crystalline. The witness sample was also used for ellipsometry measurements to derive the dielectric functions of the TiN and SiN layers. Dielectric functions of the SiN membrane and the witness sample were determined independently with ellipsometry with no attempt to confirm their stoichiometric composition.

The modeled dielectric functions of these samples were derived from fitting the ellipsometry data spanning from 400 to 40 000 cm^{-1} (0.25–25 μm) and are shown in Fig. 1. The Drude–Lorentz (DL) model consists of a parametrized Drude function and three Lorentz permittivity functions (DL). The mean squared errors of the fits are between 2 and 3, listed in the supplementary material. The fitted thicknesses are 4.4, 9.9, 11.2, and 17.3 nm for samples A, B, C, and D, respectively, and they also show a clear linear dependence with deposition time [the inset of Fig. 1(b)]. The imaginary part (ε'') of the dielectric function for all these samples is very large, as expected from a lossy material. These films are also metallic with the real part of their dielectric function (ε') being negative in most of the spectral range between 400 and 16 000 cm^{-1} (25–0.6 μm). In this thickness regime, the dielectric function is expected to be thickness dependent.[30] However, between 500 and 2500 cm^{-1} (20–4 μm), the permittivities

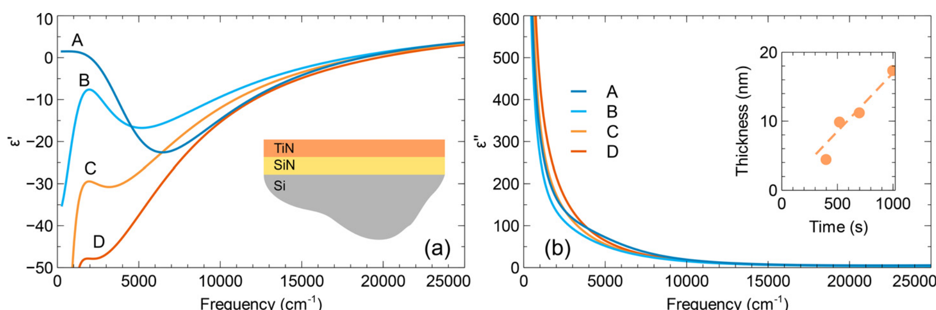

FIG. 1. Real (a) and imaginary (b) parts of the fitted permittivity function for samples A–D using the Drude–Lorentz (DL) model. Inset (a) shows the structure of the sample used for the ellipsometry measurement. Inset (b) shows the fitted thickness vs deposition time for samples A (400 s), B (525 s), C (700 s), and D (1000 s).

Published under an exclusive license by AIP Publishing

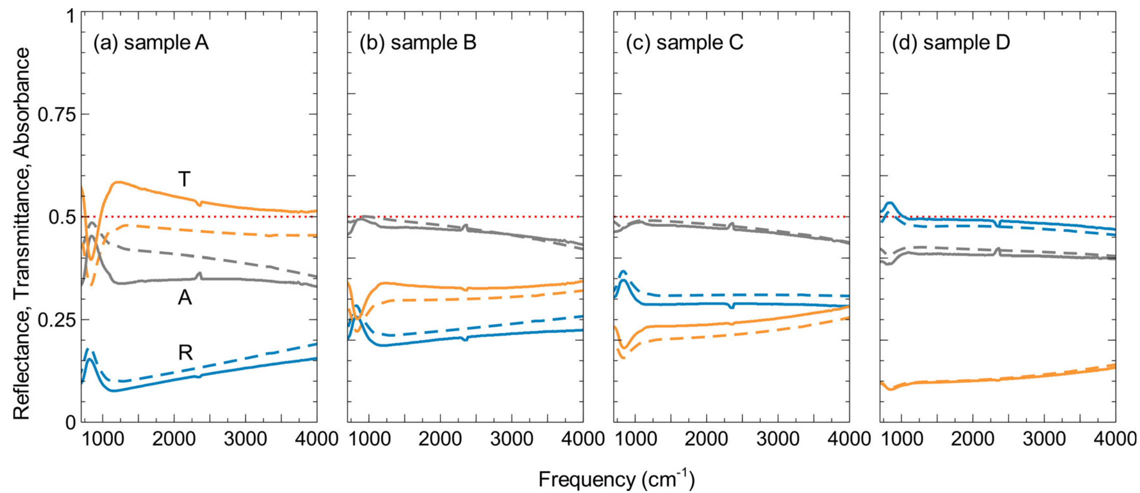

FIG. 2. Reflectance (blue), transmittance (orange), and absorptance (gray) of samples A–D, corresponding to thicknesses 4.4, 9.9, 11.2, and 17.3 nm, respectively. The dashed lines are experimental data, and the solid lines are derived from transfer matrix method (TMM) calculations using fitted dielectric functions. The red dashed line represents the maximal absorptance.

do not behave like a standard Drude model, especially for sample A. This behavior can be attributed to a Lorentz resonance at energies from 2400 to 5600 cm^{-1} (E3 = 0.3–0.7 eV in Table S1 of the supplementary material). The physical origin of this resonance is unclear as optical properties of this material in this spectral region have not been widely reported. Using an alternative dielectric function model consisting of Drude and Tauc–Lorentz permittivity functions (DTL), we can also obtain a very good fit but with the requirement of a very thin overlayer of dielectric. The presence of such a layer has been reported and interpreted as titanium oxynitride.[29,30] The derived TiN thicknesses (3–11 nm) using this model also exhibited a linear dependence with deposition time. These dielectric functions also show a similar behavior as those derived from the DL model and are shown in the supplementary material. Most importantly, these films possess the property $|\varepsilon''| \gg |\varepsilon'| \gg 1$, which is requisite for MA.

The absorptance spectra (A) of these films were obtained using spectral transmittance (T) and reflectance (R) measured with a Thermo Fisher iN10 FTIR microscope. These spectra serve as an independent validation of the dielectric functions obtained from the ellipsometry data fit and are used to evaluate the theoretical R and T spectra using TMM (Fig. 2). From these samples, as expected, the reflectance increases, and transmittance decreases with increasing thickness. For a perfectly symmetric system (i.e., in the absence of a SiN supporting film), MA occurs when the reflectance and transmittance are equal to 25%. For our non-symmetric samples, MA occurs when they are close to 25%. In addition, we found the absorptive results to be very close to each other using either DL or DTL permittivity functions.

The average experimental absorptances between 8 and 13 μm for samples A–D shown in Fig. 3(a) and are 0.39, 0.483, 0.480, and 0.4, respectively, with a standard deviation of 0.025. Within the uncertainty of the measurements, samples B and C show maximal absorptance

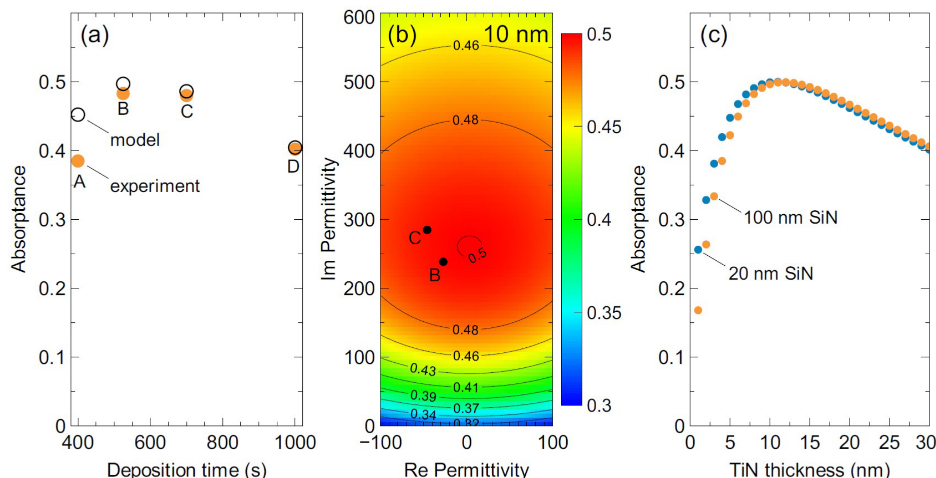

FIG. 3. (a) Measured and calculated absorptance as a function of the TiN sample thickness. (b) Calculated absorptance for various permittivity values of a 10 nm thick absorbing material supported by 100 nm of SiN. The color bar indicates absorptance with MA shown at 0.5. (c) Calculated absorptance vs TiN thickness using the permittivity function obtained from sample B for 20 and 100 nm SiN supporting films.

Published under an exclusive license by AIP Publishing

near 1000 cm^{-1} (=10 μm) in these ultrathin TiN films. Using a specific heat capacity of 0.227 J/g/°C and a density of 5.23 g/cm^3 for TiN, we obtain a thermal heat capacity of 1.2×10^{-6} J/K/cm^2 for a 10 nm film. While the absorptance of all the samples except sample A show good agreement with the TMM calculation, there are some discrepancies in the transmittance and reflectance measurements, and they become progressively larger for thinner films. We believe one of the possible sources of these discrepancies is uncertainty in the ellipsometry data, since the optical responses from the thinner films are weak. Error could also arise from actual difference in material properties between the witness sample and the film on the membrane.

While using lossy metallic films may be the simplest way to satisfy $|\varepsilon''| \gg |\varepsilon'| \gg 1$, we also considered whether such thin films need to be metallic for this condition to be achieved. To test that constraint, we used a TMM calculation to explore a broad permittivity space needed for MA for a 10 nm film supported by 100 nm of SiN. The result is presented in Fig. 3(b) which shows that MA or near-MA can be achieved within a large range of permittivity values. As previously noted,[28] the permittivity requirement for MA is rather broad. Interestingly, *the absorber material does not need to be metallic*. For the sake of visualizing where our samples B and C land on this permittivity map, they are annotated by black circles in Fig. 3(b).

In practical bolometer applications, the absorber film needs to be supported, and it is worth considering the impact of this supporting layer thickness. Including a 20 nm thick supporting SiN layer (a density of 3.2 g/cm^3, a specific heat capacity of 0.673 J/g/°C), the total heat capacity per unit area becomes 5.5 μJ/K/cm^2. The average absorptance shows a very small difference in the 8–13 μm region [Fig. 3(c)]. This confirms most absorption takes place in the TiN film. While in principle, if the absorbing structure is not symmetric, the absorptance incident from the supporting layer side can exceed the MA value of 0.5, but such an increase is very minimal unless the supporting film is very thick, too thick to be considered practical for high performance bolometer applications. Alternatively, one can increase the absorptance significantly with a back reflector and a vacuum/air spacer. Numerical calculations show that if we design an air gap of 2 μm between our sample A (the lowest absorptance measured) and a doped ($\sim 10^{20}$ cm^{-3}) Si supporting wafer, used as a reflector, then TiN and the supporting SiN structure would have an average absorptance of 0.84 in the 8–13 μm region (see the supplementary material). Incorporating this type of backplane reflector structure adds relatively minimal complication to the fabrication of a microbolometer.

In conclusion, we experimentally demonstrate MA in the IR with a 10 nm thick TiN absorber on 100 nm of SiN. We show that the permittivity requirement for MA is not limited to a metallic material as long as $|\varepsilon''| \gg |\varepsilon'| \gg 1$ is met. In addition, MA can be achieved by tuning the thickness of the TiN absorbing layer. We also present a viable fabrication method to incorporate a back reflector to enhance the absorptance of the absorber significantly.

See the supplementary material for details on thin film deposition (Fig. S1) and optical characterization of samples; expressions of dielectric functions used in the ellipsometry model; ellipsometry data and model fit of the two models used DL (Fig. S2) and DTL (Fig. S3); fitted parameters of DL model (Table S1); fitted parameters of the DTL model (Table S2); dielectric function of the TiN film obtained from the DTL model (Fig. S4); absorptance behavior with a doped Si reflector (Fig. S5); transfer matrix formalism; schematic of a microbolometer (Fig. S6) and bolometer improvement metric due to reduced thermal conductance (Fig. S7).

This work was supported by Sandia National Laboratories, Laboratory Directed Research and Development. Thin film deposition and most of the characterizations were performed at the Center for Integrated Nanotechnologies, an Office of Science, a Suer Facility operated for the DOE Office of Science. Sandia National Laboratories is a multi-mission laboratory managed and operated by National Technology and Engineering Solutions of Sandia, LLC, a wholly owned subsidiary of Honeywell International, Inc., for DOE's National Nuclear Security Administration under Contract No. DE-NA-0003525. This article describes objective technical results and analysis. The views expressed in the article do not necessarily represent the views of the DOE or the U.S. Government.

AUTHOR DECLARATIONS

Conflict of Interest

The authors have no conflicts to disclose.

Author Contributions

Ting-Shan Luk: Conceptualization (lead); Data curation (lead); Formal analysis (lead); Investigation (lead); Writing – original draft (lead); Writing – review & editing (equal). **Guangping Xu:** Resources (supporting); Writing – review & editing (equal). **Willard Ross:** Resources (supporting). **John Nogan:** Resources (supporting). **Ethan A. Scott:** Resources (equal); Visualization (equal); Writing – review & editing (equal). **Sergei Ivanov:** Resources (supporting). **Oana Niculescu:** Formal analysis (supporting); Resources (supporting). **Oleg Mitrofanov:** Formal analysis (supporting); Writing – review & editing (supporting). **Charles Thomas Harris:** Conceptualization (equal); Funding acquisition (lead); Investigation (supporting); Supervision (lead); Writing – original draft (supporting); Writing – review & editing (equal).

DATA AVAILABILITY

The data that support the findings of this study are available from the corresponding author upon reasonable request.

REFERENCES

[1]G. Gerlach and H. Budzier, *Thermal Infrared Sensors: Theory, Optimization and Practice* (Wiley, 2011).
[2]M. Michael and K.-P. Vollmer, *Infrared Thermal Imaging: Fundamentals, Research and Applications*, 2nd ed. (Wiley, 2018).
[3]Y. Ra'di, C. R. Simovski, and S. A. Tretyakov, Phys. Rev. Appl. **3**(3), 037001 (2015).
[4]A. Varpula, K. Tappura, J. Tiira, K. Grigoras, O.-P. Kilpi, K. Sovanto, J. Ahopelto, and M. Prunnila, APL Photonics **6**(3), 036111 (2021).
[5]C. Chen, C. Li, S. Min, Q. Guo, Z. Xia, D. Liu, Z. Ma, and F. Xia, Nano Lett. **21**(19), 8385 (2021).
[6]J. W. Stewart, J. H. Vella, W. Li, S. Fan, and M. H. Mikkelsen, Nat. Mater. **19**(2), 158 (2020).
[7]R. Alaee, M. Albooyeh, and C. Rockstuhl, J. Phys. D **50**, 503002 (2017).
[8]M. A. Kats and F. Capasso, Laser Photonics Rev. **10**, 735–749 (2016).
[9]Z. Wang, T. S. Luk, Y. Tan, D. Ji, M. Zhou, Q. Gan, and Z. Yu, Appl. Phys. Lett. **106**(10), 101104 (2015).

Published under an exclusive license by AIP Publishing

[10] J. Park, S. J. Kim, and M. L. Brongersma, Opt. Lett. **40**(9), 1960 (2015).
[11] Z. Li, E. Palacios, S. Butun, H. Kocer, and K. Aydin, Sci. Rep. **5**(1), 15137 (2015).
[12] H. Deng, Z. Li, L. Stan, D. Rosenmann, D. Czaplewski, J. Gao, and X. Yang, Opt. Lett. **40**(11), 2592 (2015).
[13] J. R. Piper, V. Liu, and S. Fan, Appl. Phys. Lett. **104**(25), 251110 (2014).
[14] J. Luo, S. Li, B. Hou, and Y. Lai, Phys. Rev. B **90**(16), 165128 (2014).
[15] H. Gao, C. Gu, Z. Y. Zheng, S. J. Chen, and H. Y. Hao, Appl. Phys. B **117**(3), 875 (2014).
[16] C. M. Watts, X. Liu, and W. J. Padilla, Adv. Mater. **24**(23), OP98 (2012).
[17] S. Thongrattanasiri, F. H. L. Koppens, and F. J. García de Abajo, Phys. Rev. Lett. **108**(4), 047401 (2012).
[18] T. S. Luk, S. Campione, I. Kim, S. Feng, Y. C. Jun, S. Liu, J. B. Wright, I. Brener, P. B. Catrysse, S. Fan, and M. B. Sinclair, Phys. Rev. B **90**(8), 085411 (2014).
[19] E. F. C. Driessen and M. J. A. de Dood, Appl. Phys. Lett. **94**(17), 171109 (2009).
[20] N. I. Landy, S. Sajuyigbe, J. J. Mock, D. R. Smith, and W. J. Padilla, Phys. Rev. Lett. **100**(20), 207402 (2008).
[21] C. H. Liang and X. Y. Zhao, Microwave Opt. Technol. Lett. **6**(3), 163 (1993).
[22] C. Hilsum, J. Opt. Soc. Am. **45**(2), 135 (1955).
[23] N. Liu, M. Mesch, T. Weiss, M. Hentschel, and H. Giessen, Nano Lett. **10**(7), 2342 (2010).
[24] E. Popov, D. Maystre, R. C. McPhedran, M. Nevière, M. C. Hutley, and G. H. Derrick, Opt. Express **16**(9), 6146 (2008).
[25] C. Hilsum, J. Opt. Soc. Am. **44**(3), 188 (1954).
[26] L. N. Hadley and D. M. Dennison, J. Opt. Soc. Am. **37**(6), 451 (1947).
[27] N. Luhmann, D. Høj, M. Piller, H. Kähler, M.-H. Chien, R. G. West, U. L. Andersen, and S. Schmid, Nat. Commun. **11**(1), 2161 (2020).
[28] C. Hägglund, S. P. Apell, and B. Kasemo, Nano Lett. **10**(8), 3135 (2010).
[29] C.-C. Chang, J. Nogan, Z.-P. Yang, W. J. M. Kort-Kamp, W. Ross, T. S. Luk, D. A. R. Dalvit, A. K. Azad, and H.-T. Chen, Sci. Rep. **9**(1), 15287 (2019).
[30] D. Shah, A. Catellani, H. Reddy, N. Kinsey, V. Shalaev, A. Boltasseva, and A. Calzolari, ACS Photonics **5**(7), 2816 (2018).

Published under an exclusive license by AIP Publishing